Spatial and temporal patterns of organophosphate Esters flame retardants and plasticizers in airborne particles over the Mediterranean sea

Kalliopi Violaki [a,b,*], Javier Castro-Jiménez [c], Athanasios Nenes [a,d], Richard Sempere [b], Christos Panagiotopoulos [a,b]

[a] Laboratory of Atmospheric Processes and Their Impacts, School of Architecture, Civil & Environmental Engineering, École Polytechnique Fédérale de Lausanne, Lausanne, 1015, Switzerland
[b] Aix-Marseille Univ., Université de Toulon, CNRS, IRD, MIO, Marseille, France
[c] IFREMER, Chemical Contamination of Marine Ecosystems (CCEM), Rue de L'Ile D'Yeu, BP 21105, 44311, Nantes, Cedex 3, France
[d] Center for the Study of Air Quality and Climate Change, Institute of Chemical Engineering Sciences, Foundation for Research and Technology Hellas, GR-26504, Patras, Greece

HIGHLIGHTS

- Organophosphate Esters Flame Retardants (OPEs) were associated with fossil fuel combustion and road traffic.
- Highest OPEs concentrations observed in East Mediterranean during the summer.
- OPEs peaked in North West Mediterranean during spring.
- Saharan desert influenced the concentration of Tris-(2-chloroethyl) phosphate (TCEP).

GRAPHICAL ABSTRACT
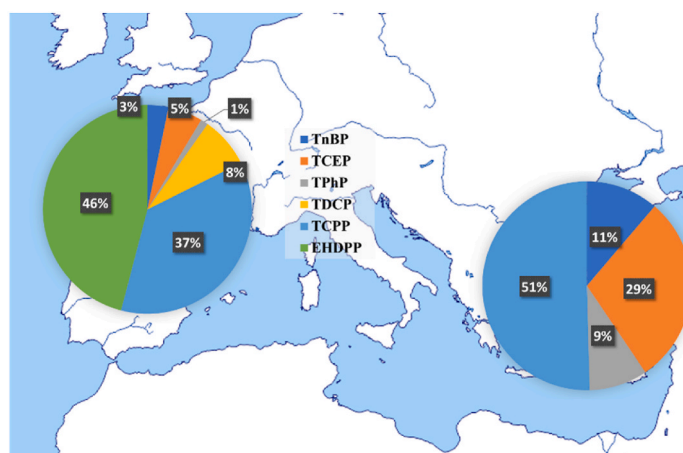
ARTICLE INFO

Handling Editor: R Ebinghaus

ABSTRACT

We studied the co-occurrence of OPEs and other constituents in atmospheric particles at the two edges of the Mediterranean Sea, under the influence of the transport of polluted air from Europe and dust from the Sahara. The highest OPE concentrations were observed during the summer period in the East Mediterranean and in spring for the NW Mediterranean. The total average atmospheric concentration of Σ_6OPEs in the NW Mediterranean was 2103 ± 2020 pg m^{-3} ($n = 23$) with EHDPP and TCPP to be the predominant OPEs, accounting on average for 46% and 37% of the total Σ_6OPEs concentrations, respectively. The average concentration of Σ_6OPEs in East Mediterranean was 156.4 ± 170.3 pg m^{-3} ($n = 67$) with TCPP showing the highest concentration (116.1

* Corresponding author. Laboratory of Atmospheric Processes and Their Impacts, School of Architecture, Civil & Environmental Engineering, École Polytechnique Fédérale de Lausanne, Lausanne, 1015, Switzerland.
E-mail addresses: kviolaki@gmail.com, kalliopi.violaki@epfl.ch (K. Violaki).

$\pm$ 92.8 pg m^{-3}), followed by TCEP (67.5 $\pm$ 55.8 pg m^{-3}). In both areas, OPEs were mostly associated with fossil fuel combustion and road traffic, while the air masses from Saharan desert influenced the concentration of EHDPP, TCEP in NW Mediterranean and the TCEP concentration levels in the East Mediterranean. The total annual deposition of reported OPEs to the Mediterranean basin was estimated to be 584 tonnes, accounting for about 8.5% of the total deposited anthropogenic phosphorus.

1. Introduction

During the last century, an increasing number of synthetic organic compounds containing phosphorus (P) have been introduced into the environment. An important class of these compounds are organophosphate triesters (OPEs) currently used in industrial and household products as plasticizers, flame retardants, and antifoaming agents (Van der Veen et al., 2012). OPEs were used as substitutes for brominated flame retardants (BFRs), especially polybrominated diphenyl ethers (PBDEs) and hexabromocyclododecanes (HBCDs) (Ren et al., 2016). OPEs are easily released into the environment due to their application as additives into the materials, where they are not chemically bound and they can be considered as contaminants of emerging concern, being detected in many environmental matrices such as water, sediment, air, indoor dust, biota, food, animals and the human body (Wong et al., 2018; Na et al., 2020; Xie et al., 2022).

Chlorinated OPEs (CL-OPEs) such as tris(1-chloro-2-propyl) phosphate (TCPP), Tris-(2-chloroethyl) phosphate (TCEP) and Tris(1,3-dichloro-2-propyl) phosphate (TDCP) exhibit a wide range of neurotoxic, immunotoxic, and carcinogenic effects in laboratory animal experiments (Van der Veen et al., 2012). TDCP is harmful when inhaled and can easily enter the bloodstream affecting the hormone system in infants (Percy et al., 2021). TCEP is toxic to aquatic organisms (Wu et al., 2017), and has adversely impacts to human health (Chen et al., 2015) leading to hemolytic and reproductive effects. Furthermore, the non-CL-OPEs have also harmful health and environmental impacts e.g., tri-n-butyl phosphate (TnBP) could be neurotoxic (Chen et al., 2020; Kung et al., 2022), 2-ethylhexyl diphenyl phosphate (EHDPP) is expected to partition mostly in the particulate phase in the atmosphere (Kung et al., 2022) and is suspected to be carcinogenic as it was found in elevated concentrations in the plasma of women diagnosed with tumors (Liu et al., 2021). Moreover, an unrecognized risk for urban populations worldwide involves the exposure to OPEs photooxidation products (Liu et al., 2021). Over hundred transformation products detected from common OPEs e.g., TCEP, TCPP, TDCP, TPhP, EHDPP, TEHP can be up to tenfold more toxic and persistent than the parent chemicals (Liu et al., 2021).

OPEs are released to the atmosphere directly by volatilization from industrial and household products (Wei et al., 2015), and are adsorbed onto atmospheric particles where they can be transported over long distances before deposition. OPEs, as plastic additives, are believed to be secondarily released to the atmosphere from micro and nano plastics (Bhat et al., 2023). OPEs have been widely detected in the atmosphere over the oceans with concentrations ranged from few pg to 4400 pg m^{-3} with TCPP, TnBP and EHDPP being predominant (Moeller et al., 2012; Castro-Jiménez et al., 2016; Saini et al., 2020). Higher OPEs atmospheric concentrations have been reported over urban and industrial areas (Saini et al., 2020) ranging from few hundreds of pg to 15,100 pg m^{-3}. Indoor air can contain exceedingly high levels of OPEs, up to 330, 000 pg m^{-3} especially in office spaces (Wong et al., 2018).

Most of OPEs have been measured mainly in marine regions of the northern hemisphere, with TCPP be the predominant component and TnBP recorded only in samples influenced by continental air masses (Castro-Jiménez et al., 2016). Despite that the importance of OPEs in the aquatic environment as organic pollutants has been widely recognized (Xie et al., 2020) further research is warranted particularly on atmospheric deposition of anthropogenic P originated from OPEs and its potential use as a nutrient source in large oligotrophic marine areas, such as the Mediterranean Sea. This area is influenced seasonally by the Saharan dust storms, burdening the atmosphere with millions of tonnes of dust annually (Guerzoni, et al., 1999), together with summertime wildfire episodes, wintertime domestic wood burning and polluted air masses from northern and central Europe. These airborne particles can also transport OPEs, among other organic pollutants, leading to their atmospheric deposition to Mediterranean basin. The occurrence of atmospheric particle-associated OPEs over the Mediterranean Sea has been reported in only two studies; one during cruise measurements across Mediterranean (Castro-Jiménez et al., 2014) and the second in NW African Mediterranean coastal area (Castro-Jiménez et al., 2018). However, regional characterization using identical sampling and analysis approaches have not been carried out before. This is addressed in this study by analyzing, six widely occurring OPEs including TCPP, TDCP, TCEP, TnBP, TPhP, EHDPP in total suspended atmospheric particles (TSP) collected from the North West and East Mediterranean atmosphere. The OPEs sources were investigated in the study area by using the approach of source-trace indicators analyzed in the same samples with OPEs. The spatial and temporal patterns, the atmospheric deposition of OPEs and the biogeochemical implications of anthropogenic P deposition are then discussed.

2. Materials and methods

2.1. Study areas and sampling

Aerosol samples ($n = 67$) were collected over one-year period starting from October 2016 (Fig. S1) in the northern front of the University of Crete in Greece, (35° 18′ N, 25°45′ E), in the East Mediterranean (East Med.) a semirural site approximately 6 km far from the city of Heraklion. Aerosol samples ($n = 23$) were collected from February to July 2018 in North West Mediterranean (NW Med.) on the roof top of the MIO lab (Luminy Campus; 43°14′7.16″N, 5°26′26.58″E), a semirural site in the middle of a pine forest and approximately 15 km from the Marseille city center (Fig. S1).

Aerosol samples were collected at both sites on a precombusted (450 °C for 6 h) Pallflex quartz fiber filter (QFF 20 × 25 cm; Pall, 2500QAT-UP) using a high-volume air sampler (TISCH) with a 48 h sampling resolution and at flow rate of 85 m^3 h^{-1}. The filters were wrapped in the pre-combusted aluminum foil and stored in double-sealed plastic bags in a freezer at −20 °C before processing.

2.2. Chemical analysis

For OPEs analysis, QFF sub-samples (~32 cm^2) were extracted in 4 mL of ethyl acetate by sonicating for 60 min. The extracts were centrifuged at 5000 g for 10 min and the supernatants were injected , after 5 times dilution in methanol and addition of D7-Malathion (CAS: 352,438-94-9) as internal standard, with final concentration in each sample 1 μg L^{-1}. The analysis was performed by LC-ESI-Q-TOF/MS coupling an Agilent 1290 Infinity LC and an Agilent 6530 Accurate-Mass Q-TOF systems.

The chromatographic separation was performed with an Eclipse Plus (Agilent) column (50mm × 2.1 mm I.D., 1.8 μm particle size). The gradient chromatographic separation was achieved by using as mobile phase H$_2$O with 5 mM ammonium acetate (A) and acetonitrile with 5 mM ammonium acetate (B). The gradient elution was: 1) 10% (A) from 0 to 2.5 min, 2) 50% (A) from 2.5 to 12 min, 3) 10% (A) from 12 to 17

min. A representative chromatograph was presented in Fig. S2. The flow rate was set at 100 μL min^{-1}. The column temperature was set at 25 °C and a 2 μL volume injection was used. The ionization was performed in positive mode using the following operational parameters: capillary voltage, 3500 V; drying gas, 8 L min^{-1}; nebulizer pressure, 35 psig; Gas temperature 350 °C, sheath gas temperature, 300 °C; sheath gas flow, 11 L min^{-1}; nozzle voltage, 1000 V; fragmentor voltage, 160 V; skimmer voltage, 65 V and octopole RF, 750 V. The full scan MS data were recorded at a rate of 1 spectrum s^{-1} for *m/z* 50–1700 at 2 GHz. All the MS data were recorded with Agilent Mass Hunter Data Acquisition (B.05.00) and processed by Agilent Mass Hunter Qualitative Analysis (B.05.00). The samples were analyzed for the following OPEs: **1)** tris-(2-chloroethyl) phosphate (TCEP; CAS: 115-96-8), **2)** tris[2-chloro-1-(chloromethyl) ethyl] phosphate (TDCP; CAS: 13,674-87-8), **3)** tris-(1-chloro-2-propyl) phosphate (TCPPs, mix of isomers; CAS: 13,674-84-5), **4)** tris-n-butyl phosphate (TnBP; CAS: 126-73-8), **5)** triphenyl phosphate (TPhP; CAS: 115-86-6), **6)** 2-ethylhexyl diphenyl phosphate (EHDPP; CAS: 1241-94-7).

Additional complementary analysis of trace metals and main ions were performed in the same samples. The details of the analysis are described in the SI.

2.3. Quality assurance/quality control (QA/QC)

The limits of OPEs detection (LODs) were calculated as a S/N ratio = 3 on the lowest standards used for calibration and ranged from 0.2 to 1 ppb. LODs ranged from 0.01 to 0.18 μg L^{-1} and those were converted to atmospheric concentrations by dividing them with the average sampling volume in m^3 (0.1–2.3 pg m^{-3}) (Table S1). To evaluate the method recoveries, standard addition experiments were performed in triplicate by spiking a mixture of analyzed OPEs on a clean QFF and extracted as indicated above. Results confirm the good recoveries of our method; with an average OPEs recovery of 90 ± 14% (Table S2). Results were not corrected by recoveries. Field blanks (*n* = 8) were performed by placing QFFs in the filter holder from sampler and then dismounted and stored (with no air pumped through) as the real samples. Field blanks were below LODs except from TCPP, and EDHPP which exhibited average values of 32% and 4% of the average measured in samples, respectively. Results were blank corrected by subtracting the average field blank values.

3. Results and discussion

3.1. Detection frequency and spatial distribution of OPEs

Targeted OPEs were found in all samples collected in the NW Med. (100% detection frequency, DF), except for TnBP which was slightly lower (96%; Fig. S3). The total average atmospheric concentration of $\sum_6$OPEs was 2103 ± 2020 pg m^{-3}. EHDPP and TCPP were the predominant OPEs over NW Med., with relative abundance at 46% and 37% to the total $\sum_6$OPEs, respectively (Table S11). The other target OPEs represented a minor relative contribution: TDCP (8%), TCEP (5%), TnBP (3%) and TPhP (1%) of the total $\sum_6$OPEs concentrations. EHDPP presents the highest average concentration (1148 ± 1529 pg m^{-3}, Table 1) of all OPEs. A high DF was observed in the East Med. only for TCEP (100%) and TPhP (91%). The rest of OPEs exhibited a lower DF, ranging from 0% or not detected (TDCP and EHDPP) to 75% (TnBP). The average concentration of $\sum_6$OPEs was 156.4 ± 170.3 pg m^{-3}. Among the detected OPEs, the TCPP presented the highest relative abundance (50%) but with low DF (46%, Fig. S3), followed by TCEP (29%, Table S11) with average concentration at 67.5 ± 55.8 pg m^{-3} (Table 1).

3.2. Seasonal pattern of OPEs over NW and East Mediterranean

NW Mediterranean. Overall higher concentrations ($\sum_6$OPEs) were found in spring (3412 pg m^{-3}), followed by summer (1400 pg m^{-3}) and

Table 1
Atmospheric concentration in pg m^{-3} of OPEs measuring in East and NW Mediterranean. In brackets are presented the values [median, min, max], zero values were not included.

OPEs	East Med. (n = 67)	North West Med. (n = 23)
TCPP (mix isomers)	116.1 ± 92.8 [98.3, 6.2, 346.0]	609.9 ± 402.1 [594.6, 85.1, 1677]
TCEP	67.5 ± 55.8 [51.8, 4.6, 235.6]	89.3 ± 88.4 [81.0, 12.0, 399.4]
TDCP	n.d	149.1 ± 80.8 [144.4, 40.2, 407.6]
TnBP	25.8 ± 22.1 [21.1, 0.1, 87.7]	55.3 ± 57.2 [27.5, 7.7, 194.9]
TPhP	20.8 ± 17.5 [17.7, 0.8, 99.5]	21.3 ± 21.1 [12.1, 5.2, 94.6]
EHDPP	n.d	11801 ± 1555 [499.5, 174.3, 6518]
$\sum_6$OPEs	230.2	2106

winter (941.4 pg m^{-3}). Total OPEs concentrations in spring and winter were clearly driven by EHDPP values. This compound is used as an additive in plastics, especially in food packaging and hydraulic fluids (Wei et al., 2015), while it is accumulated partially on fine particles (d < 2.5 μm) (Liu et al., 2014), promoting its long-range transport. TCPP was the second most abundant CL-OPE in spring (646.3 ± 485.3 pg m^{-3}, Fig. 1) but peaked during summer (751.6 ± 274.1 pg m^{-3}, Fig. 1). The predominance of TCPP had been previously reported for the marine atmosphere of the Mediterranean and Black Sea (Castro-Jiménez et al., 2014), in aerosol phase samples collected from the tropical and subtropical Atlantic, Pacific, and Indian Ocean (Castro-Jiménez et al., 2016), but also in urban areas (Saini et al., 2020) or remote marine environments e.g., Arctic (Salamova et al., 2014). It had also been reported that TCPP represents approximately 80% of the CL-OPEs in Europe (Castro-Jiménez et al., 2014), and is by production volume the most widely used OPE. A significant correlation was found (*r* = 0.71, *p* < 0.05, Table S3) between TCPP and Al during summer suggesting the transport via dust particles (Marconi et al., 2014). The correlation of TCPP with Zn (*r* = 0.71, *p* < 0.05, Table S3) suggested their co-existence with emissions from urban industrialized areas and road traffic (Querol et al., 2007), while the significant correlation with non-sea salt K$^+$ (nss-K$^+$) (*r* = 0.83, *p* < 0.05, Table S3) suggested their mixing with biomass burning emissions (Reid et al., 2005), this could be especially true when during biomass burning events apart from vegetations burning are included also the burning of houses, cars or other urban installations containing OPEs compounds.

The second abundant CL-OPEs was TDCP, with average summer concentration of 175.4 ± 55.3 pg m^{-3} (Fig. 1), presented significant correlation with non-sea salt Ca^{2+} (nss-Ca^{2+}) (*r* = 0.74, *p* < 0.05, Table S3), indicating an association with dust particles (Marconi et al., 2014). But TDCP was mostly correlated with anthropogenic tracers such as V (*r* = 0.76, *p* < 0.05, Table S3) and Ni (*r* = 0.81, *p* < 0.05, Table S3) suggesting the co-existence with fossil fuel combustion (e.g., ships in harbors) but also was correlated with Cr (*r* = 0.71, *p* < 0.05, Table S3), Zn (*r* = 0.65, *p* < 0.05, Table S3) and As (*r* = 0.68, *p* < 0.05, Table S3), suggesting their co-existence with emissions from urban industrialized areas (Querol et al., 2007, Zhao et al., 2021).

The non CL-OPEs exhibited higher average summer concentration were EHDPP (373.0 ± 156.4 pg m^{-3}) and TnBP (21.0 ± 12.3 pg m^{-3}) following by TPhP (10.6 ± 3.1 pg m^{-3}). EHDPP and TPhP presented significant correlation with Al (*r* = 0.60, *p* < 0.05, and *r* = 0.79, *p* < 0.05, respectively, Table S3) suggesting dust-associated sources (Marconi et al., 2014). In addition, TPhP was correlated with anthropogenic emissions tracers such as V (*r* = 0.63, *p* < 0.05, Table S3), Ni (*r* = 0.69, *p* < 0.05, Table S3) and Zn (*r* = 0.73, *p* < 0.05, Table S3) suggesting an association with the fossil fuel combustion and road traffic with TPhP emissions (Querol et al., 2007).
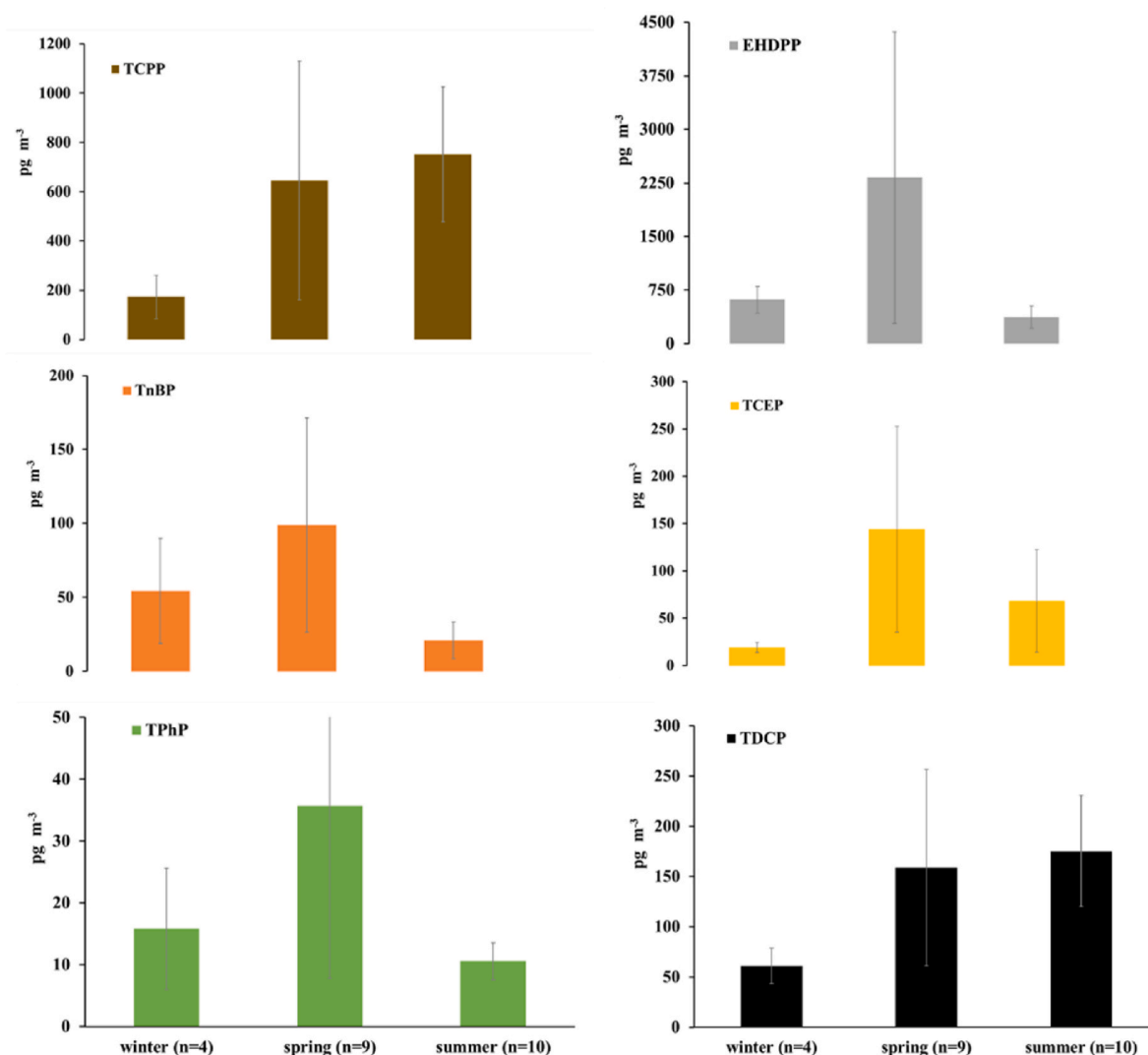
Fig. 1. Seasonal variation of OPEs detected in atmospheric particles in the NW Mediterranean during the sampling period (Feb. to Jul. 2018). Error bars represent the standard deviation. As winter season was considered the months February, spring the months March, April and May and summer June and July.

During winter the most abundant OPEs were the EHDPP (617.2 ± 187.1 pg m^{-3}) and TCPP (173.8 ± 87.9 pg m^{-3}). EHDPP ($r = 0.78$, $p < 0.05$, Table S4), TCPP ($r = 0.82$, $p < 0.05$, Table S4), TDCP ($r = 0.80$, $p < 0.05$, Table S4) and TPhP ($r = 0.83$, $p < 0.05$, Table S4), TnBP ($r = 0.72$, $p < 0.05$, Table S4) were correlated with V confirming the contribution of fossil fuel combustion. TnBP was also correlated with Na ($r = 0.74$, $p < 0.05$, Table S4) and Cl ($r = 0.74$, $p < 0.05$, Table S4) proposing the mixture with sea salt particles. EHDPP presented significant correlation with almost all variables measured in spring (Table S5) proposed a complex mixture of atmospheric material during this period, however the number of samples was low ($n = 5$).

The HYSPLIT (Hybrid Single Particle Lagrangian Integrated Trajectory) trajectory model was used to simulate the five-day air mass back trajectories in 1000 m and 3000 m (Stein et al., 2015). During the sampling period three main domains were prevailed; air masses from Northwest and central France, polluted and industrialized East and central Europe, Saharan dust and marine (Fig. S6). Air masses from the Saharan desert and marine sources influenced the concentration of EHDPP and TCEP increasing their average concentration by 30% and 16 %, respectively (Table S6). EHDPP emission increased also when winds from North and central France prevailed, however no significance change was observed for the other OPEs compounds.

East Mediterranean. All OPEs peaked in summer (Σ_6OPEs = 321.3

pg m^{-3}) and presented lower concentration during winter (Σ_6OPEs = 39.9 pg m^{-3}, Fig. 2), likely due to rain wash out. Temperature may also affect emissions of OPEs, being larger from land and water as temperature increases (Castro-Jiménez et al., 2018). This is consistent with their higher levels found in summer (average T = 26 ± 3 °C) and autumn (average T = 21 ± 4 °C) in this study (Fig. 2) and a similar study in West Mediterranean (Castro-Jiménez et al., 2018). Additionally, the indoor dust is a significant source for the most OPEs (Wong et al., 2020) compounds in the outdoor environment. This is especially true during the summer period when observed higher exchange rates between indoor and outdoor air (Zhao et al., 2020).

Higher TCPP concentrations were observed during autumn (76.8 ± 55.3 pg m^{-3}) and summer (168.5 ± 109.8 pg m^{-3}). TCPP is accumulated mainly in fine mode (d $<$ 2.5 μm) and with lifetime ranged from 0.5 to 20 days, depending on atmospheric conditions (Li et al., 2017a) promoted the long-range transport. Significant correlation of TCPP was observed with V ($r = 0.57$, $p < 0.05$, Table S7) and Ni ($r = 0.52$, $p < 0.05$, Table S7) in summer suggesting their association with fossil fuel combustion (Querol et al., 2007), while in autumn a significant correlation with Al ($r = 0.51$, $p < 0.05$, Table S8) pointing to the transport with dust particles.

Higher TCEP concentrations were observed during autumn (84.3 ± 34.9 pg m^{-3}) and summer (88.0 ± 75.7 pg m^{-3}). TCEP was significantly
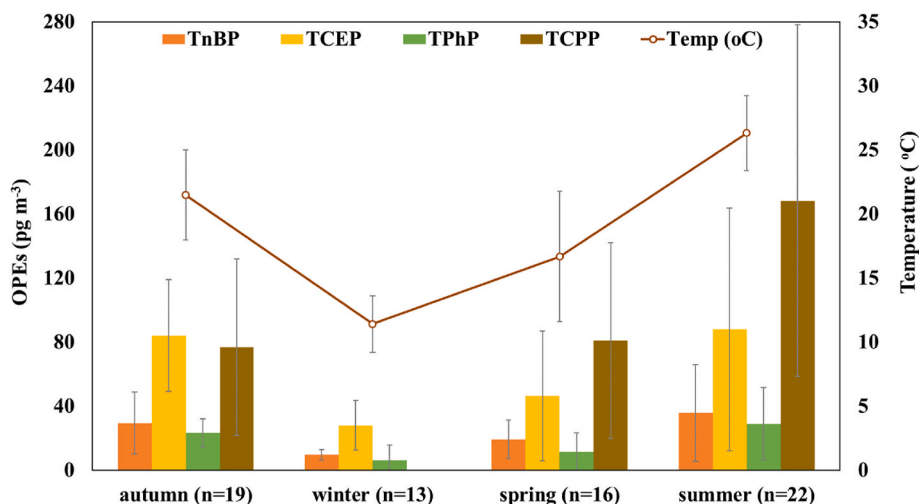
Fig. 2. Seasonal variation of OPEs detected in atmospheric particles in the East Mediterranean, during the sampling period (Oct. 2016–Sep. 2017). Error bars represent the standard deviation. Temperature data were obtained from the weather stations NOANN network described in Lagouvardos et al. (2017).

correlated with V ($r = 0.57$, $p < 0.05$, Table S7) and Cu ($r = 0.45$, $p < 0.05$, Table S7), suggesting the contribution of fossil fuel combustion and road traffic (Querol et al., 2007) in summer, while in autumn correlated with Al ($r = 0.71$, $p < 0.05$, Table S8) and nss-calcium ($r = 0.69$, $p < 0.05$, Table S8) confirming their mixture with dust. Sühring et al. (2020) proposed 36 days of persistence in the air for TCEP, supporting the transport from remote sources. TCEP was replaced by TCPP in Europe, however TCEP was still detected as the dominant OPE in the atmosphere e.g., in the atmosphere of northeast Atlantic and the Arctic Ocean (Li et al., 2017b).

Higher TnBP concentrations recorded during autumn (29.4 ± 19.3 pg m^{-3}) and summer (35.9 ± 30.2 pg m^{-3}) suggest that local sources potentially contribute to the OPEs emissions during those seasons, since TnBP presents the shortest lifetime ($t_{1/2}(h) < 1$) (Wei et al., 2015). Furthermore, TnBP was correlated significantly with As ($r = 0.55$, $p < 0.05$, Table S8) during autumn, pointing to a contribution from the local urban industrialized area (Querol et al., 2007). Finally, higher TPhP concentrations recorded during autumn (23.4 ± 8.6 pg m^{-3}) and summer (29.0 ± 22.7 pg m^{-3}) together with significant correlation with V ($r = 0.63$, $p < 0.05$, Table S7) and Cu ($r = 0.60$, $p < 0.05$, Table S7), suggest the association with fossil fuel combustions and road traffic in summer (Querol et al., 2007), and in autumn with Al ($r = 0.59$, $p < 0.05$, Table S8) and nss-Ca^{2+} ($r = 0.49$, $p < 0.05$, Table S8), as expected for their mixture with dust.

The HYSPLIT trajectory model was used to simulate the five-day air mass back trajectories for 1000 m and 3000 m during the sampling period. Three main air masses were identified including Sahara desert, the polluted Black Sea, and industrialized central Europe (Violaki et al., 2021). The air mass origin has no significant influence to the concentration of OPEs except the TCEP concentration levels (Table S12), which seems to be influenced by the Saharan dust transport (85.2 ± 48.6 pg m^{-3}), increasing their ambient average concentration by up to 30%. This is in agreement with the significant correlation with Al and nss-Ca^{2+} observed in spring and autumn when the dust events are more frequent. Slightly increased concentrations were recorded during dust events for TnBP (29.5 ± 17.6 pg m^{-3}) and TPhP (22.5 ± 15.8 pg m^{-3}).

3.3. Atmospheric deposition of OPEs and environmental implications

To evaluate the atmospheric dry deposition of OPEs, we estimated the deposition velocity (V_d) of each OPE since it depends on the aerosol size distribution (Spokes et al., 2001), but also can be dramatically influenced by pollution or dust episodes (Koçak et al., 2016). The settling velocities for each species can be estimated as follows: $V_d = (C_c$

$\times 2.0) + (C_f \times 0.1)$, where C_c and C_f are the relative contribution of coarse and fine modes; 2.0 and 0.1 cm s^{-1} are the deposition velocities (Koçak et al., 2016) for coarse and fine aerosols, respectively. The size distribution of each OPE were calculated based on the size segregated aerosol samples ($n = 2$), which they were collected in the East Mediterranean (SI, section 1.1). The impactor separated the particles in five different stages: from larger than 7.2 μm to less than 0.49 μm (Fig. S4). Assuming as fine fraction the particles with diameter d < 1.5 μm and coarse the particles with d > 1.5 μm we calculated the V_d for the each OPE (Table S13) and then the deposition fluxes were calculated based on the equation: F $= -V_d$ C, where F is the OPEs flux in pg m^{-2} s^{-1}, C is the atmospheric concentration of OPEs in pg m^{-3} and V_d is the deposition velocity in m s^{-1}. EHDPP presented a bimodal distribution while all the rest OPEs were accumulated mostly in fine mode (Fig. S4). The estimated deposition velocity ranged from 0.1 cm s^{-1} to 1.1 cm s^{-1}, (av. 0.3 $\pm$ 0.4 cm s^{-1}) being in the range proposed by the Lao et al. (2022). The monthly variation of OPEs daily depositions in both areas was estimated based on the above (Fig. 3). The average daily deposition rates of Σ_6OPEs in East Med. was 18.7 ± 13.6 ng m^{-2} d^{-1}, while higher deposition rates were reported during dry season starting from April to September (Violaki et al., 2018), maximizing in June (46.9 ng m^{-2} d^{-1}). The East Med. is particularly nutrient starved during that period, however the more toxic CL-OPEs are prevalent. The average daily deposition rates of Σ_6OPEs in NW Med. was 1436 ± 1430 ng m^{-2} d^{-1}, while higher deposition rates were reported in April (3586 ng m^{-2} d^{-1}). The dominance of EHDPP is remarkable with average daily deposition during the sampling period at 1333 ± 1388 ng m^{-2} d^{-1}, contributing with 92% to total OPEs deposition due mainly to its bimodal distribution.

The hypothesis that OPEs could serve as source of organic P upon deposition for marine micro-organisms has been recently investigated experimentally (Vila-Costa et al., 2019). These authors reported that the biodegradation of OPEs can have a direct impact on our understanding of the biogeochemical cycle of P in seawater. According to their work, OPEs can be used as a source of P under limiting conditions, since the alkaline phosphatase could assimilate the P ester bond in bioavailable P. The Mediterranean Sea is considered as a low-nutrient, low-chlorophyll marine environment where bacterioplankton experience P limitation and phytoplankton experience co-limitation by nitrogen and phosphorus in the summer (Krom et al., 2005; Pitta et al., 2005) and hence the role of OPEs upon deposition will be investigated.

In order to estimate the deposition fluxes as P released from OPEs, we considered the number of P atoms in each OPE molecule. The average dry deposition of P from OPEs in the East Med. was estimated at 2.0 ± 1.4 ng P m^{-2} d^{-1} (range: 0.5–4.9 ng P m^{-2} d^{-1}), yielding an annual dry
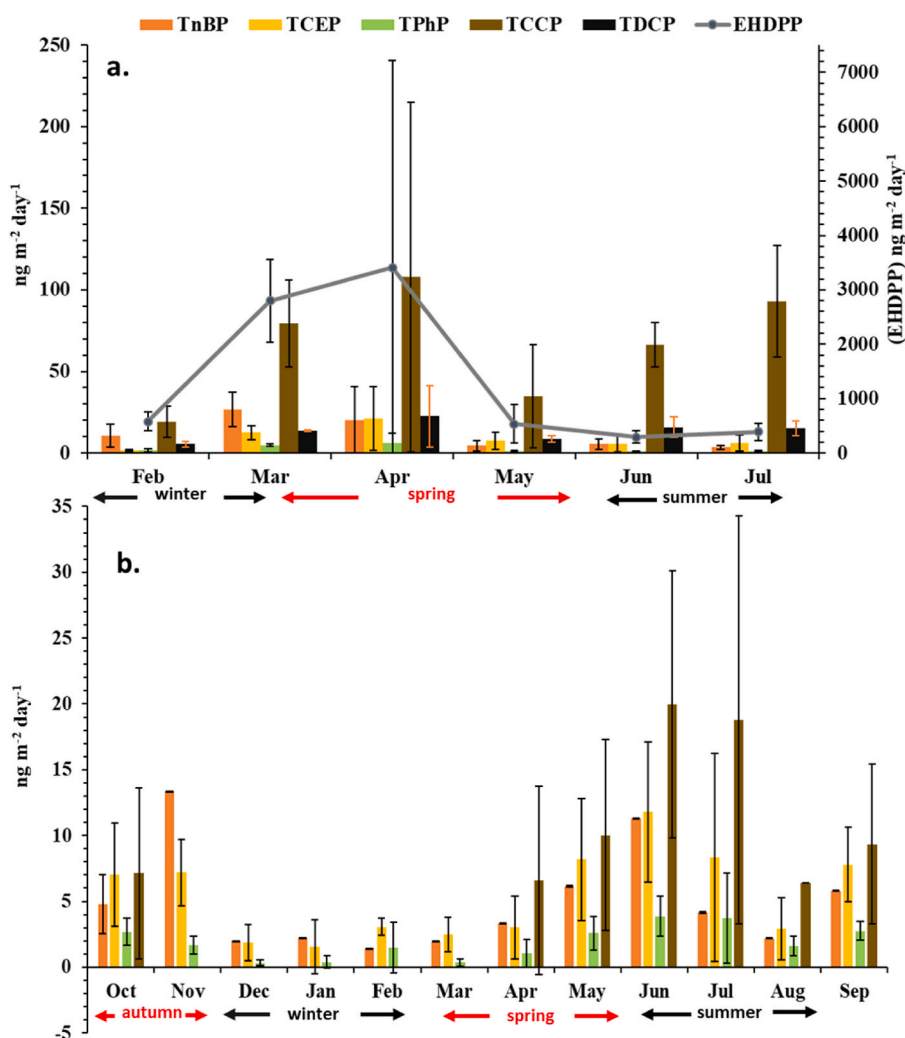
Fig. 3. Monthly variation of OPEs daily deposition in the a) NW Mediterranean during the sampling period (Feb. to Jul. 2018) and b) East Mediterranean during the sampling period (Oct. 2016–Sep. 2017). As winter season was considered the months from December to February, spring the months from March to May and summer from June to August. Error bars represent the standard deviation.

deposition flux of 0.7 ± 0.5 μg P m^{-2} y^{-1}. Higher atmospheric deposition fluxes of OPEs as P were estimated in the NW Med., with an average value of 123.7 ± 122.6 ng P m^{-2} d^{-1} (range: 51.0–308.0 ng P m^{-2} d^{-1}), yielding an annual dry deposition of P at 45.2 ± 44.7 μg P m^{-2} y^{-1}. For comparison, these estimates are similar of those performed for the open Mediterranean Sea based on cruise sampling of the atmospheric particle phase (average of 40 ng P m^{-2} d^{-1}) (Castro-Jiménez et al., 2014). However, the fact that a theoretical average deposition velocity of 0.2 cm s^{-1} was used for all samples and the number for OPEs was higher ($\sum_{14}$OPEs) can make this comparison difficult.

Extrapolating the calculated P fluxes to the Mediterranean surface (Candela, et al., 1989) and acknowledging the uncertainty due to the low number of sampling sites, the annual dry deposited P due to measured OPEs to the Mediterranean basin was estimated at 50 tonnes of P. Considering the annual deposited total P for Mediterranean basin (Kanakidou et al., 2020) as 62.3 Gg-P y^{-1}, and considering as anthropogenic the 11% of this (Violaki et al., 2021) the percentage contribution of OPEs in anthropogenic P pool could be at 8.5%. We consider this as a lower-end estimate because wet deposition is not included in this study. In addition, the diffusive deposition of OPEs derived from atmospheric gas-phase concentrations, estimated to be 2–3 orders of magnitude larger than dry deposition in other oligotrophic marine environments (Castro-Jiménez et al., 2016), and is not considered.

4. Conclusions

The co-occurrence of OPEs with other components of atmospheric particles, as source-trace indicators, at two edges of Mediterranean Sea indicate that both the NW and East Med. basins are influenced by the transport of polluted air masses from north and central Europe, but also from Saharan dust episodes reaching high TCEP levels. The highest concentrations were recorded during the summer period in the East Med. while in the NW Med. was recorded during spring. The latter is justified from the presence of EHDPP with higher concentrations during Saharan dust transportation, which happens more often in the spring. The total concentration of OPEs in NW Med. was 57 times higher than the East area, while the total annual deposition of targeted OPEs to the Mediterranean basin was estimated to 584 tonnes. The implications of the OPE-induced increased of the anthropogenic P pool in the Mediterranean Sea are still unknown, but should be one of the research priorities for the next future due do the massive global used of these plastic additives with the lack of a sound regulatory framework. In addition, more research is needed on the occurrence and the chemical identification of OPEs transformation products, which are an unrecognized exposure risk for the environment as was underlined recently in the literature.

Authors statements

K·V.: conceptualization, methodology, writing- Original draft preparation. K.V., J.J. collected and analyzed data. K.V., C·P: resources. KV, R.S. and A.N., have funding acquisition. A.N., J.J., R.S., C.P. Reviewing and Editing.

Declaration of competing interest

The authors declare that they have no known competing financial interests or personal relationships that could have appeared to influence the work reported in this paper.

Data availability

Data will be made available on request.

Acknowledgments

Appendix A. Supplementary data

Supplementary data to this article can be found online at https://doi.org/10.1016/j.chemosphere.2023.140746.

References

Bhat, M.A., Gedik, K., Gaga, E.O., 2023. Atmospheric micro (nano) plastics: future growing concerns for human health. Air Qual. Atmos. Health 16, 233–262. https://doi.org/10.1007/s11869-022-01272-2.

Candela, J., Winant, C.D., Bryden, H.L., 1989. Meteorologically Forced sub inertial flows through the Strait of Gibraltar. J. Geophys. Res. 94, 12667–13664 12679. https://doi.org/10.1029/JC094iC09p12667.

Castro-Jiménez, J., Sempéré, R., 2018. Atmospheric particle-bound organophosphate ester flame retardants and plasticizers in a North African Mediterranean coastal city (Bizerte, Tunisia). Sci. Total Environ. 642, 383–393. https://doi.org/10.1016/j.scitotenv.2018.06.010.

Castro-Jimenez, J., Berrojalbiz, N., Pizarro, M., Dachs, J., 2014. Organophosphate ester (OPE) flame retardants and plasticizers in the open Mediterranean and Black seas atmosphere. Environ. Sci. Technol. 48, 3203–3209. https://doi.org/10.1021/es405337g.

Castro-Jimenez, J., et al., 2016. Organophosphate ester flame retardants and plasticizers in the global oceanic atmosphere. Environ. Sci. Technol. 50, 12831–12839. https://doi.org/10.1021/acs.est.6b04344.

Chen, G., Jin, Y., Wu, Y., Liu, L., Fu, Z., 2015. Exposure of male mice to two kinds of organophosphate flame retardants (OPFRs) induced oxidative stress and endocrine disruption. Environ. Toxicol. Pharmacol. 40, 310–318. https://doi.org/10.1016/j.etap.2015.06.021.

Chen, Y.Y., Song, Y.Y., Chen, Y.J., Zhang, Y.H., Li, R.J., Wang, Y.J., Qi, Z.H., Chen, Z.F., Cai, Z.W., 2020. Contamination profiles and potential health risks of organophosphate flame retardants in $PM_{2.5}$ from Guangzhou and Taiyuan, China. Environ. Int. 134, 105343 https://doi.org/10.1016/j.envint.2019.105343.

Guerzoni, S., Chester, R., Dulac, F., Herut, B., Loÿe-Pilot, M.-D., Measures, C., Migon, C., Molinaroli, E., Moulin, C., Rossini, P., Saydam, C., Soudine, A., Ziveri, P., 1999. The role of atmospheric deposition in the biogeochemistry of the Mediterranean Sea. Prog. Oceanogr. 44, 147–190. https://doi.org/10.1016/S0079-6611(99)00024-5.

Kanakidou, M., Myriokefalitakis, S., Tsagkaraki, M., 2020. Atmospheric inputs of nutrients to the Mediterranean Sea. Deep Sea Res. Part II Top. 171, 104606 https://doi.org/10.1016/j.dsr2.2019.06.014.

Koçak, M., Mihalopoulos, N., Tutsak, E., Violaki, K., Theodosi, C., Zarmpas, P., Kalegeri, P., 2016. Atmospheric Deposition of Macronutrients (Dissolved Inorganic Nitrogen and Phosphorous) onto the Black Sea and Implications on Marine Productivity, 2016, pp. 1727–1739. https://doi.org/10.1175/JAS-D-15-0039.1.

Krom, M.D., Woodward, E.M.S., Herut, B., Kress, N., Carbo, P., Mantoura, R.F.C., Spyres, G., Thingstad, T.F., Wassmann, P., Wexels-Riser, C., Kitidis, V., Law, C.S., Zodiatis, G., 2005. Nutrient cycling in the south east Levantine basin of the eastern Mediterranean: results from a phosphorus starved system. Deep Sea Res. Part II 52, 2879–2896. https://doi.org/10.1016/j.dsr2.2005.08.009.

Kung, H.C., Hsieh, Y.K., Huang, B.W., Cheruiyot, N.K., Chang-Chien, G.P., 2022. An overview: organophosphate flame retardants in the atmosphere. Aerosol Air Qual. Res. 22, 220148 https://doi.org/10.4209/aaqr.220148.

Lagouvardos, K., Kotroni, V., Bezes, A., Koletsis, I., Kopania, T., Lykoudis, S., Mazarakis, N., Papagiannaki, K., Vougioukas, S., 2017. The automatic weather stations NOANN network of the National Observatory of Athens: operation and database, 2017 Geosci. Data J. 4, 4–16.

Lao, J.-Y., Lin, H., Qin, X., Ruan, Y., Leung, K.M.Y., Zeng, E.Y., Lam, P.K.S., 2022. Insights into the atmospheric persistence, transformation, and health implications of organophosphate esters in urban ambient air. Environ. Sci. Technol. 56 (17), 12003–12013. https://doi.org/10.1021/acs.est.2c01161.

Li, C., Chen, J., Xie, H.-B., Zhao, Y., Xia, D., Xu, T., Li, X., Qiao, X., 2017a. Effects of atmospheric water on ·OH-initiated oxidation of organophosphate flame retardants: a DFT investigation on TCPP. Environ. Sci. Technol. 51 (9), 5043–5505. https://doi.org/10.1021/acs.est.7b00347, 1.

Li, J., Xie, Z., Mi, W., Lai, S., Tian, C., Emeis, K.-S., Ebinghaus, R., 2017b. Organophosphate esters in air, snow, and seawater in the North Atlantic and the Arctic. Environ. Sci. Technol. 51, 6887–6896. https://doi.org/10.1021/acs.est.7b01289.

Liu, Y., Huang, L., Li, S.-M., Harner, T., Liggio, J., 2014. OH-initiated heterogeneous oxidation of tris-2-butoxyethyl phosphate: implications for its fate in the atmosphere. Atmos. Chem. Phys. 14, 12195–12207. https://doi.org/10.5194/acp-14-12195-2014.

Liu, Q., Li, L., Zhang, X., et al., 2021. Uncovering global-scale risks from commercial chemicals in air. Nature 600, 456–461. https://doi.org/10.1038/s41586-021-04134-6.

Marconi, M., Sferlazzo, D.M., Becagli, S., Bommarito, C., Calzolai, G., Chiari, M., di Sarra, A., Ghedini, C., Gómez-Amo, J.L., Lucarelli, F., Meloni, D., Monteleone, F., Nava, S., Pace, G., Piacentino, S., Rugi, F., Severi, M., Traversi, R., Udisti, R., 2014. Saharan dust aerosol over the central Mediterranean Sea: PM10 chemical composition and concentration versus optical columnar measurements. Atmos. Chem. Phys. 14, 2039–2054. https://doi.org/10.5194/acp-14-2039-2014.

Moeller, A., Sturm, R., Xie, Z., Cai, M., He, J., Ebinghaus, R., 2012. Organophosphorus flame retardants and plasticizers in airborne particles over the northern pacific and Indian ocean toward the polar regions: evidence for global occurrence. Environ. Sci. Technol. 46, 3127–3134. https://doi.org/10.1021/es204272v.

Na, G., Hou, C., Li, R., Shi, Y., Gao, H., Jin, S., Gao, Y., Jiao, L., Cai, Y., 2020. Occurrence, distribution, air-seawater exchange and atmospheric deposition of organophosphate esters (OPEs) from the Northwestern Pacific to the Arctic Ocean. Mar. Pollut. Bull. 157, 111243 https://doi.org/10.1016/j.marpolbul.2020.111243.

Percy, Z., Vuong, A.M., Xu, Y., Xie, C., Ospina, M., Calafat, A.M., Hoofnagle, A., Lanphear, B.P., Braun, J.M., Cecil, K.M., 2021. Maternal urinary organophosphate esters and alterations in maternal and neonatal thyroid hormones. Am. J. Epidemiol. 190, 1793–1802. https://doi.org/10.1093/aje/kwab086.

Pitta, P., Stambler, N., Tanaka, T., Zohary, T., Tselepides, A., Rassoulzadegan, F., 2005. Biological response to P addition in the Eastern Mediterranean Sea. The microbial race against time. Deep Sea Res. Part II 52, 2961–2974. https://doi.org/10.1016/j.dsr2.2005.08.012.

Querol, X., Viana, M., Alastuey, A., Amato, F., Moreno, T., et al., 2007. Source origin of trace elements in PM from regional background, urban and industrial sites of Spain. Atmos. Environ. 41 (34), 7219–7231. https://doi.org/10.1016/j.atmosenv.2007.05.022.

Reid, J.S., Koppmann, R., Eck, T.F., Eleuterio, D.P., 2005. A review of biomass burning emissions part II: intensive physical properties of biomass burning particles. Atmos. Chem. Phys. 5, 799–825. https://doi.org/10.5194/acp-5-799-2005.

Ren, G., Chen, Z., Feng, J., Ji, W., Zhang, J., Zheng, K., Yu, Z., Zeng, X., 2016. Organophosphate esters in total suspended particulates of an urban city in East China. Chemosphere 164, 75–83. https://doi.org/10.1016/j.chemosphere.2016.08.090.

Saini, A., Harner, T., Chinnadhurai, S., Schuster, J.K., Yates, A., Sweetman, A., Aristizabal-Zuluaga, B.H., Jiménez, B., Manzano, C.A., et al., 2020. GAPS-megacities: a new global platform for investigating persistent organic pollutants and chemicals of emerging concern in urban air. Environ. Pollut. 267, 115416 https://doi.org/10.1016/j.envpol.2020.115416.

Salamova, A., Hermanson, M.H., Hites, R.A., 2014. Organophosphate and halogenated flame retardants in atmospheric particles from a European Arctic site. Environ. Sci. Technol. 48, 6133–6140. https://doi.org/10.1021/es500911d.

Spokes, L.J., Jickells, T.D., Jarvis, K., 2001. Atmospheric inputs of trace metals to the northeast Atlantic Ocean: the importance of southeasterly flow. Mar. Chem. 76, 319–330. https://doi.org/10.1016/S0304-4203(01)00071-8.

Stein, A.F., Draxler, R.R., Rolph, G.D., Stunder, B.J.B., Cohen, M.D., Ngan, F., 2015. " NOAA's HYSPLIT atmospheric transport and dispersion modeling system". Bull. Am. Meteorol. Soc. 96 (12), 2059–2077. https://doi.org/10.1175/BAMS-D-14-00110.1.

Sühring, R., Scheringer, M., Rodgers, T.F.M., Jantunen, L.M., Diamond, M.L., 2020. Evaluation of the OECD POV and LRTP screening tool for estimating the long-range transport of organophosphate esters. Environ. Sci.: Process. Impacts 22, 207–216. https://doi.org/10.1039/C9EM00410F.

Van der Veen, I., de Boer, J., 2012. Phosphorus flame retardants: properties, production, environmental occurrence, toxicity and analysis. Chemosphere 88 (10), 1119–1153. https://doi.org/10.1016/j.chemosphere.2012.03.067.

Vila-Costa, M., Sebastián, M., Pizarro, M., Cerro-Gálvez, E., Lundin, D., Gasol, J.M., Dachs, J., 2019. Microbial consumption of organophosphate esters in seawater under phosphorus limited conditions. Sci. Rep. 9, 233. https://doi.org/10.1038/s41598-018-36635-2.

Violaki, K., Nenes, A., Tsagkaraki, M., et al., 2021. Bioaerosols and dust are the dominant sources of organic P in atmospheric particles. npj Clim. Atmos. Sci. 4, 63. https://doi.org/10.1038/s41612-021-00215-5.

Wei, G.L., Li, D.Q., Zhuo, M.N., Liao, Y.S., Xie, Z.Y., Guo, T.L., Li, J.J., Zhang, S.Y., Liang, Z.Q., 2015. Organophosphorus flame retardants and plasticizers: sources, occurrence, toxicity and human exposure. Environ. Pollut. 196, 29–46. https://doi.org/10.1016/j.envpol.2014.09.012.

Wong, F., de Wit, C.A., Newton, S.R., 2018. Concentrations and variability of organophosphate esters, halogenated flame retardants, and polybrominated diphenyl ethers in indoor and outdoor air in Stockholm, Sweden. Environ. Pollut. 240, 514–522. https://doi.org/10.1016/j.envpol.2018.04.086.

Wu, Y., Su, G., Tang, S., Liu, W., Ma, Z., Zheng, X., Liu, H., Yu, H., 2017. The combination of in silico and in vivo approaches for the investigation of disrupting effects of tris (2-chloroethyl) phosphate (TCEP) toward core receptors of zebrafish. Chemosphere 168, 122–130. https://doi.org/10.1016/j.chemosphere.2016.10.038.

Xie, Z., Wang, P., Wang, X., Castro-Jimenez, J., Kallenborn, R., Liao, C., Mi, W., Lohmann, R., Vila-Costa, M., Dachs, J., 2022. Organophosphate ester pollution in the oceans. Nat. Rev. Earth Environ. 3, 309–322. https://doi.org/10.1016/j.scitotenv.2020.139071.

Zhao, J., Birmili, W., Wehner, B., Daniels, A., Weinhold, K., Wang, L., Merkel, M., Kecorius, S., Tuch, T., Franck, U., Hussein, T., Wiedensohler, A., 2020. Particle mass concentrations and number size distributions in 40 homes in Germany: indoor-to-outdoor relationships, diurnal and seasonal variation. Aerosol Air Qual. Res. 20, 576–589. https://doi.org/10.4209/aaqr.2019.09.0444.

Zhao, J., Zhang, Y., Xu, H., Tao, S., Wang, R., Yu, Q., et al., 2021. Trace elements from ocean-going vessels in East Asia: vanadium and nickel emissions and their impacts on air quality. J. Geophys. Res. Atmos. 126, e2020JD033984 https://doi.org/10.1029/2020JD033984.